Materials Research Proceedings 44 (2024) 691-697 https://doi.org/10.21741/9781644903254-74

Development of joining technology between FeCrAl alloys and fusion reactor piping materials

KANAI Ryui[1,a *], NAOKO Oono[1,b], INAO Daisuke[2,c], NAGASAKA Takuya[3,d] and HOKAMOTO Kazuyuki[2,e]

[1]Yokohama National University, 79-5 Tokiwadai, Hodogaya-ku, Yokohama 240-8501, Japan

[2]Kumamoto University, 2-39-1 Kurokami, Chuo-ku, Kumamoto-shi 860-8555, Japan

[3]National Institute for Fusion Science,322-6 Oroshicho, Toki 509-5202, Japan

[a]kanai-ryui-nr@ynu.ac.jp, [b]oono-naoko-yh@ynu.ac.jp, [c]inao@tech.kumamoto-u.ac.jp, [d]nagasaka.takuya@nifs.ac.jp, [e]hokamoto@mech.kumamoto-u.ac.jp

Keywords: Clad Materials, Intermediate Products, Bonding Distance

Abstract. The use of FeCrAl alloys as an inner lining for piping materials for fusion reactors is being considered. The FeCrAl alloy/SUS316L joints were explosion welded to avoid the influence of an oxide film at the joint interface. The joint length could be increased by increasing the charge ratio or reducing the material thickness. Together with the microstructure observation, hardness test, 4-point bending test and heat treatment test results, it is clear that explosion welding is suitable for joining FeCrAl-ODS and SUS316L.

Introduction

FeCrAl alloys have excellent corrosion resistance due to the formation of a protective alumina film by pre-oxidation treatment and are therefore suitable for the liners used in highly corrosive environments, such as liquid metal breeder blanket piping with operating temperatures above 500°C [1]. However, since fusion reactor designs require low activation elements, the addition of non-low activation Al is problematic [2]. In addition, the high temperature strength of the tubes cannot be maintained with ferritic FeCrAl alloys alone [3], and powder metallurgy strengthened versions of FeCrAl alloys are expensive to produce. We are considering clad materials of FeCrAl alloys with current structural material candidates to provide answers to the above issues. Welding is undesirable because it alters the microstructure of the thin pipe material (a few mm to 10 mm is assumed in some designs [2,4]) in fusion reactors under thermal effects. Solid phase diffusion bonding is difficult to apply to FeCrAl alloys due to the formation of a protective alumina film at high temperatures. Explosion welding is a joining method that produces very few intermediate products and can join a wide range of dissimilar metals without losing the characteristics of each metal, because a gaseous metal splash (metal jet) produced in front of the point of impact blows away oxides films and allows contact between the newly formed metal surfaces [5]. In this study, FeCrAl alloys are bonded to SUS316L fusion reactor pipe material by explosion welding and their bondability is tested.

Experimental Methods

Two types of FeCrAl alloys were selected: Kanthal® APMT, a commercial FeCrAl alloy, and FeCrAl based oxide dispersion strengthened alloy (FeCrAl-ODS). Table 1 shows the composition of these alloys and SUS316L. For the FeCrAl alloys, test specimens for explosion welding were cut out from the ingots. For SUS316L, pre-cut pieces were purchased. The dimensions of APMT and FeCrAl-ODS were 40 mm long x 11 mm wide x 3 mm thick and 40 mm long x 14.9 mm wide x 3 mm thick respectively; the dimensions of SUS316L were 180 mm long x 100 mm wide with varying thicknesses of 2 mm and 3 mm. The specimen surfaces were polished to a roughness of

less than 1 μ m using an automatic polishing machine (Buehler EcoMet250) prior to the explosion welding.

Table 1. Composition of APMT, SUS316L and FeCrAl-ODS [wt.%].

Elements	Fe	Cr	Al	Ni	Mo	Ti	Zr	Y_2O_3
APMT[11]	balance	21	5	—	3.0	—	—	—
FeCrAl-ODS	balance	15	7	—	—	0.5	0.4	0.5
SUS316L	balance	18	—	12	2.5	—	—	—

Explosion welding was performed using facilities at the Institute of Industrial Nanomaterials, Kumamoto University. The test layout is shown in Fig. 1. A SUS316L flyer plate was installed on the upper side, and FeCrAl-ODS or APMT as a cover plate on the lower side. The explosives used was ammonium nitrate-based explosive (PAVEX manufactured by Kayaku Japan Co., Ltd., whose explosion velocity, and density are approximately 2.4 km/s and 530 kg/m3, respectively), and acrylic resin (13 mm) spacers were inserted at the four corners to ensure impact velocity. The details of the test conditions are given in Table 3. The charge ratio is expressed as the weight of the explosive per the weight of flyer plate. For example, in the case of a 3 mm SUS316L plate, the charge ratio of 0.81 corresponds to an explosive weight of 350 g.

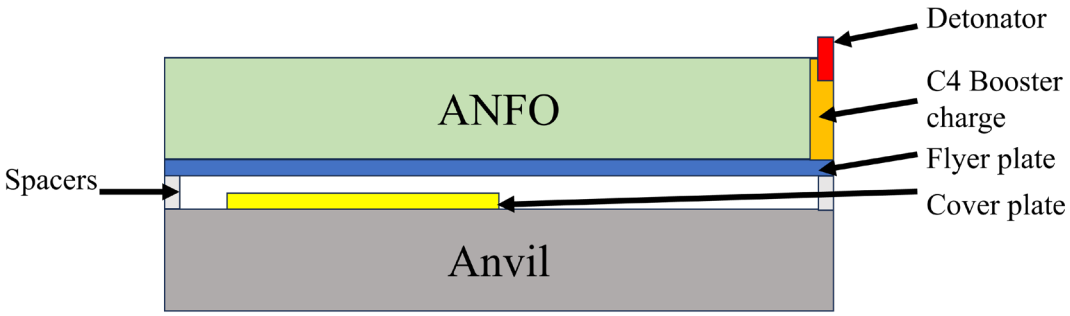

Fig. 1. Layout of explosion welding.

Table 2. Charge ratio and SUS316L thickness.

		Thickness of SUS316L [mm]	Charge ratio	Number of sheets	Number of tests
(a)	APMT	3	0.81	1	2
(b)	APMT	3	0.95	1	4
(c)	FeCrAl-ODS	2	1.43	1	2
(d)	FeCrAl-ODS	2	1.63	1	2
(e)	FeCrAl-ODS	3	0.95	1	1
(f)	FeCrAl-ODS	3	1.09	1	2

After explosion welding, the specimens were evaluated by cross-sectional microstructure observation, hardness testing and four-point bend testing. For the cross-sectional observation, the specimen cross-sections were polished to a roughness of less than 1μm as described above and observed using an optical microscope to measure the length of connection sections (hereafter referred to as "bonding length"). Scanning electron microscope (SEM) observation was also used to determine the morphology and bonding state of the interface. A micro-Vickers hardness test

was carried out using the Akashi MVK-E to investigate the hardness distribution near the interface with a test load of 9.8 N and a holding time of 15 sec. The distance from the interface and the diagonal length of the imprints were measured using a polarizing telescope (Nicon ECLIPSE ME600). The four-point bending test was performed using equipment at the National Institute for Fusion Science (NIFS). Three bending specimens with the dimensions shown in Fig. 2 were obtained from one APMT explosion welding specimen. The specimens were tested at a displacement rate of 0.20 mm/min in the bending direction at room temperature.

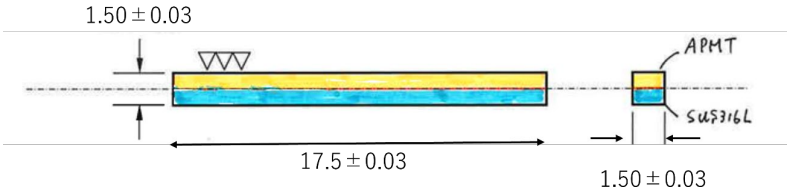

Fig. 2. 4-point bending specimen dimensions.

Results and Discussion

Fig. 3 shows the relationship between the bonding length and the number of explosives (listed as charge ratio). The bonding length of 0.0 refers to the one that was peeled off after the test.

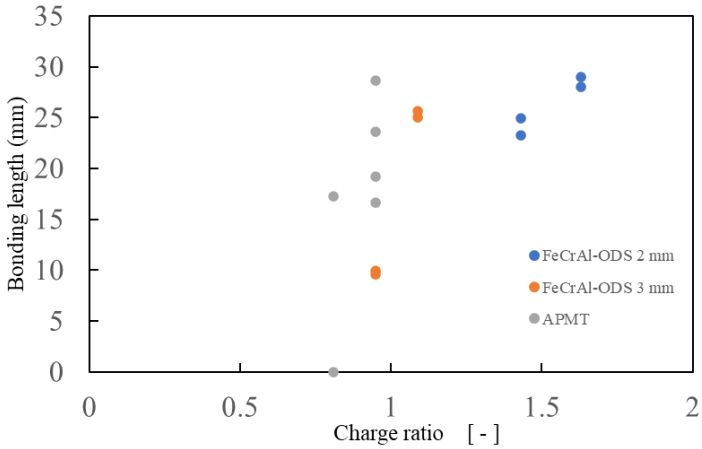

Fig. 3. Relation between charge ratio and bonding length.

As shown in Fig. 3, the bonding length increases with increasing the charge ratio and decreasing the thickness of the flyer plate (SUS316L). It can be interpreted that the charge ratio and plate thickness contribute to an increase in the velocity of the impact. For the same charge ratio, bonding length becomes shorter in the APMT/SUS316L joints than in the FeCrAl-ODS/SUS316L joints. The Vickers hardness of SUS316L is 200 HV [6], that of APMT is 250 HV [7], and that of FeCrAl-ODS is 326 HV [8]. During explosion welding, the metal jets produced cause an enormous deformation at very high strain rates on the surfaces being joined, and this is the origin of the bonding. The stress required for this deformation depends on the yield stress and work hardening coefficient of the materials being welded [9]. The stress is provided by the pressure of the jet generated between the joined materials; in other words, stiffer (harder to deform) materials require higher impact velocities. The exact work hardening coefficients of the FeCrAl alloys used in this work are not available, but the 0.2% proof stress of APMT and FeCrAl-ODS at room temperature are 510 to 600 MPa [7] and 887MPa [10] at room temperature, respectively. It can therefore be said that FeCrAl-ODS requires an even higher charge ratio or a thinner cover plate than APMT.

Cross-sectional views of the bonded interfaces by optical microscope are shown in Fig. 4. In all images, the upper side of the figure shows APMT or FeCrAl-ODS, and the lower side shows

SUS316L. Comparisons between (a) and (b), (c) and (d), (e) and (f), the shape of the wave tip (surrounded by the red lines) grows into a hook shape for larger charging ratios. The tips of the waves appear to have areas of different color from both FeCrAl and SUS316L. From the SEM energy-dispersive spectroscopy (EDS), there were no oxide films at the interfaces (map not shown).

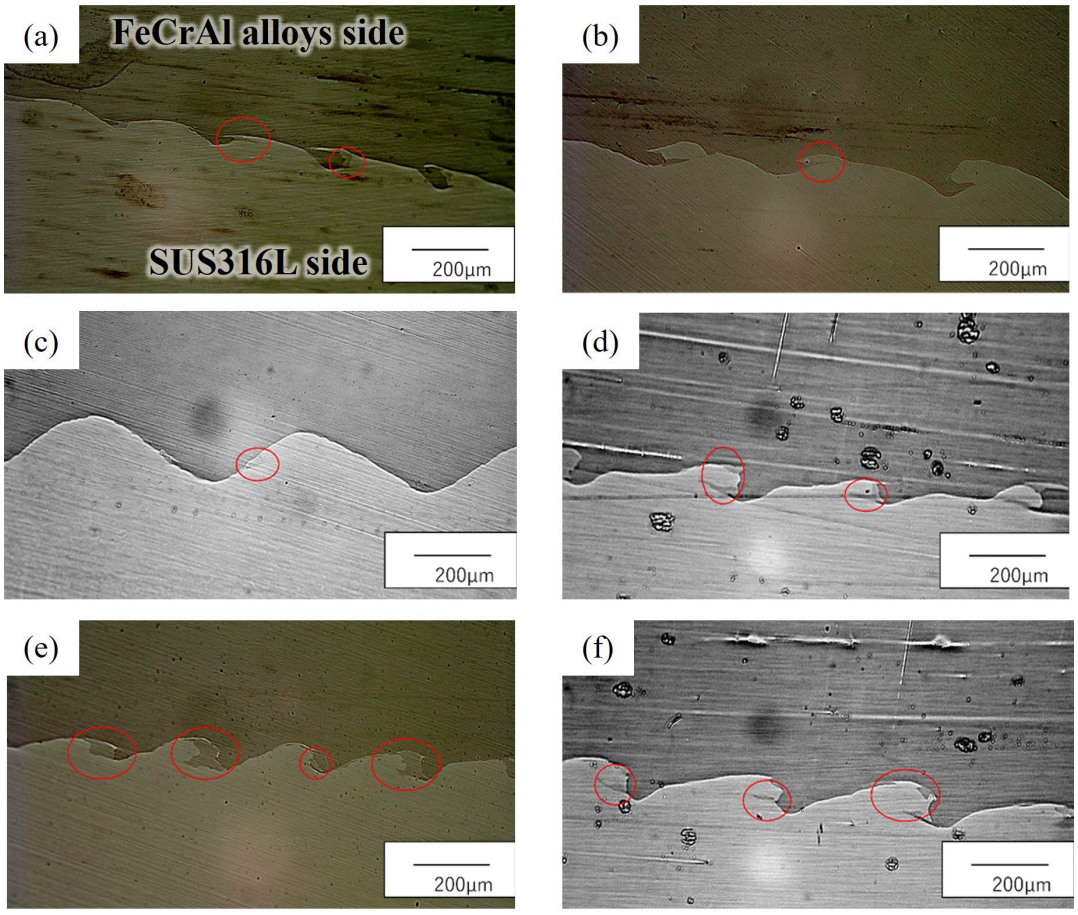

Fig. 4. Optical microscope of the bonding interfaces: (a) APMT charge ratio 0.81 (b) APMT charge ratio 0.95 (c) FeCrAl-ODS SUS316L 2mm charge ratio 1.43 (d) FeCrAl-ODS SUS316L 2mm charge ratio 1.63 (e) FeCrAl-ODS SUS316L 3mm charge ratio 0.95 (f) FeCrAl-ODS SUS316L 3mm charge ratio 1.09.

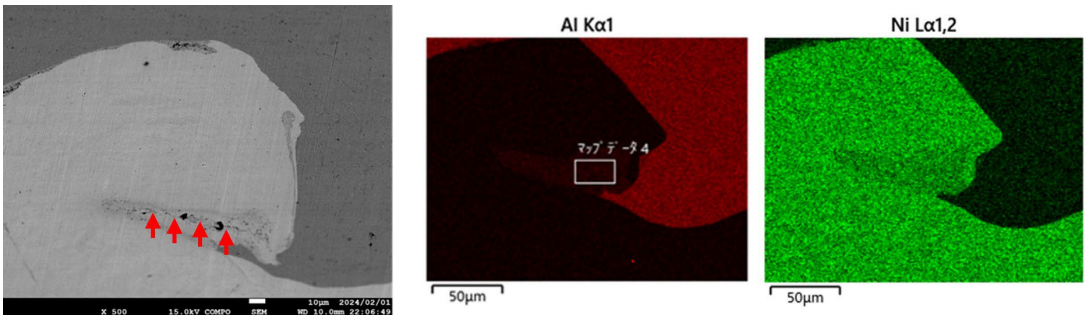

Fig. 5. SEM COMPO image of the bonding interface under the condition (f) and EDS elemental maps of Al and Ni at the same position.

Fig. 5 shows the detailed SEM COMPO image at the wave tip of the joint under the condition (f) in Fig. 4 and its Al and Ni elemental maps obtained by EDS. Al or Ni diffusion near the interface was negligible. From the EDS maps, Al and Ni coexist in intermediate products in the area of different color in the optical microscope (corresponding to the area surrounded by a rectangle in the Al map), indicating the molten portions of the FeCrAl-ODS and SUS316L. In addition, cracks were observed in this area (indicated by arrows in the SEM COMPO image). The same phenomenon occurred under conditions (c) and (e). In the molten area, Al, a ferrite-stabilizing element, and Ni, an austenite-stabilizing element, coexist, and the crystal structure changes from the austenite phase at high temperature immediately after solidification to the ferrite or martensite phase as the temperature decreases, which may cause local cracking. On the other hand, in condition (d), the presence of a molten zone was also confirmed but no cracks were observed (image not shown).

Fig. 6 shows the Vickers microhardness distribution across the bonding interface under condition (b) and (f). As a comparison, the original hardness of SUS316L, APMT, and FeCrAl-ODS are drawn as lines on the graph. In both conditions, the hardness increase nearby the bonding interface and become even higher than the original materials. This trend was observed to varying degrees in all conditions. The main possible cause for this is severe deformation at the interface during explosion welding: as can be seen in Fig. 4, the joint interface has a severe wave shape, clearly indicating that significant plastic deformation has occurred during joining. Martensitic transformation in the molten area, as described above, can also affect the hardness of the interface. Fig.7 shows the layout of the indentation.

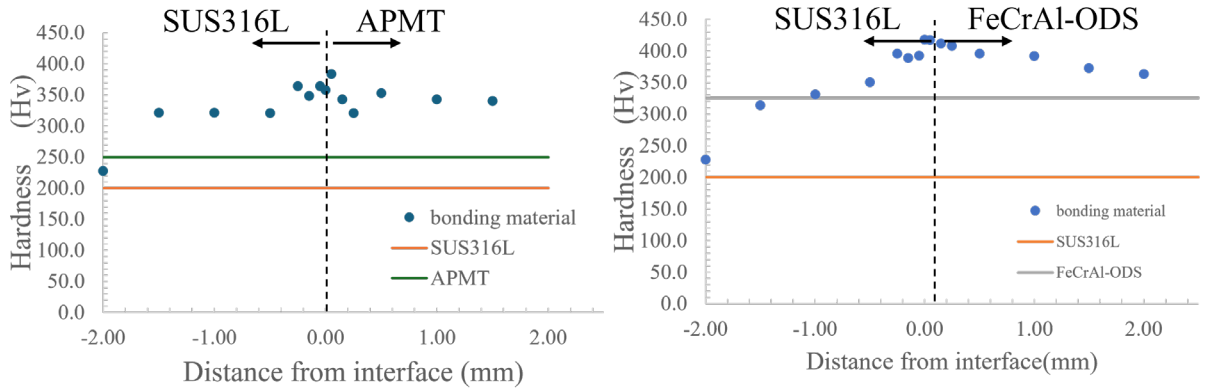

Fig. 6. Hardness changes in the vicinity of the bonding interface under condition (b) (left) and (f) (right) in Table 2.

Fig. 7. The layout of the indentation.

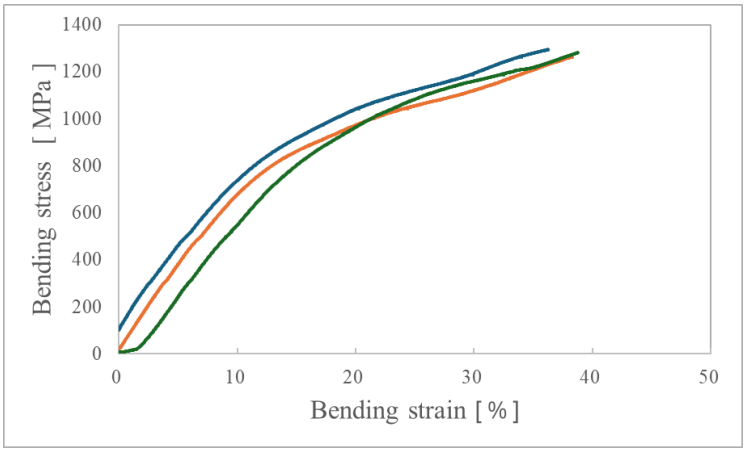

Fig. 8. Stress-strain diagram of bending test.

Fig. 8 shows stress-strain diagrams from the 4-point bending test. Stresses were calculated from the equation in the literature [11]. No interface failure was observed after the test. From Fig. 7, the first yield was observed at a bending stress of approximately 800 MPa. The bending strength of SUS316L is reported to be 896 MPa [12], which is similar to the results of this experiment. As the bending strength of APMT is not known, a comparison is made using 0.2% proof stress. The proof stress of SUS316L is 175 MPa [8] at room temperature. Since SUS316L is weaker than APMT (the proof stress of APMT was described above), the first yielding should be caused by SUS316L. It can be said that the joint strength is sufficient for explosion welding, although the possibility that the interface strength up to specimen fracture needs to be investigated cannot be ruled out. As measurement is impossible due to the design of the 4-point bending test, this will be a future issue, including the development of a suitable test.

Conclusions

Explosion welding was performed between two types of FeCrAl alloys (APMT and FeCrAl-ODS) and SUS316L. The following conclusions were drawn from the analysis.

(1) The joint length of the explosion weld joint depends on the amount of explosive and the thickness of the flyer plate. In the case of FeCrAl-ODS, a good joint length and a crack-free joint interface were obtained as the thickness of SUS316L decreased and the charge ratio increased.

(2) Cross-sectional observation at the bonding interface showed intermediate products at the interface; SEM-EDS analysis confirmed that these products were molten portions of the base metal and mating material. Cracks were observed in the molten portions in some of the joint specimens.

(3) Hardening was observed in the vicinity of the interface, but this did not affect the fracture origin during 4-point bending test. No fracture was observed at the interface, and the yield was observed at about 800 MPa. Therefore, it can be said that a good joint material was obtained in this test range.

Acknowledgements

Explosion welding was funded and supported by the Joint Usage/Research, the Institute of Industrial Nanomaterials, Kumamoto (K2023-19). The SEM microanalysis was supported by the Instrumental Analysis Center at Yokohama National University. 4-point bending test was funded and supported by the NIFS Collaboration Research program (NIFS23KIEF047) and NINS program of Promoting Research by Networking among Institutions (Grant Number 01412302).

References

[1] M. Kondo, S. Hatakeyama, N. Oono, T. Nozawa, Corrosion-resistant materials for liquid LiPb fusion blanket in elevated temperature operation, *Corros. Sci.* **197** (2022) 110070. https://doi.org/10.1016/j.corsci.2021.110070

[2] T. Tanaka, T. Chikada, T. Hinoki, T. Muroga, Electrical insulation performances of ceramic materials developed for advanced blanket systems under intense radiations, J. Nucl. Mater. 569 (2022) 153917. https://doi.org/10.1016/j.jnucmat.2022.153917

[3] M.S. Burton, Metallurgical Principles of Metal Bonding, Welding-J 11 (1954) 1051.

[4] R. Nishio, T. Tanaka, N. Oono, M. Kondo, Reduction of MHD pressure drop by electrical insulating oxide layers in liquid breeder blanket of fusion reactors, Nucl. Mater. Energy 34 (2023) 101382. https://doi.org/10.1016/j.nme.2023.101382

[5] T. Fujio, Explosion Welding, Japan Weld. Soc. 41 (1972) 28-33.

[6] https://www.toyo-success.co.jp/product/characteristic_s.html

[7] https://www.kanthal.com/en/products/material-datasheets/tube/kanthal-apmt/

[8] S. Ukai, K. Sakamoto, S. Ohtsuka, S. Yamashita, A. Kimura, Alloy design and characterization of a recrystallized FeCrAl-ODS cladding for accident-tolerant BWR fuels: An overview of research activity in Japan, J. Nuclear Mater. 583 (2023) 154508. https://doi.org/10.1016/j.jnucmat.2023.154508

[9] Y. Ma, T. Wang, G. Wang, X. Fang, C. Chu, Numerical and experimental studies of the interface characteristics and wave formation mechanism of Hastelloy/stainless steel explosive welding composite plate, *Mater. Today Commun.* **36** (2023) 106880. https://doi.org/10.1016/j.mtcomm.2023.106880

[10] P. Dou, Z.-X. Xin, W. Sang, A. Kimura, Age-hardening mechanisms of 15Cr ODS ferritic steels with 5, 7 and 9 wt.% Al at 475°C for 9000 h, J. Nucl. Mater. 540 (2020) 152368. https://doi.org/10.1016/j.jnucmat.2020.152368

[11] H. Fu, T. Nagasaka, T. Muroga, W. Guan, S. Nogami, H. Serizawa, S. Geng, K. Yabuuchi, A. Kimura, Plastic deformation behavior and bonding strength of an EBW joint between 9Cr-ODS and JLF-1 estimated by symmetric four-point bend tests combined with FEM analysis, Fusion Eng. Des. 102 (2016) 88-93. https://doi.org/10.1016/j.fusengdes.2015.11.037

[12] https://www.silicolloy.co.jp/characteristic/mechanical2/